Smart fire-safety cotton fabric with fire-warning capability via dual working mechanisms

Tao Zou
South China University of Technology
Dongqiao Zhang (simonbridgezdq@gmail.com)
Guangzhou University
Tao Xu
Guangzhou University
Xiaohong Peng
South China University of Technology
He Zhang
South China University of Technology
Yanliang Du
Guangzhou University

Research Article

Keywords: cotton fabric, fire warning, dual working mechanisms, temperature sensing, fire safety

Posted Date: December 14th, 2022

DOI: https://doi.org/10.21203/rs.3.rs-2356510/v1

Additional Declarations: No competing interests reported.

Version of Record: A version of this preprint was published at Cellulose on May 9th, 2023. See the published version at https://doi.org/10.1007/s10570-023-05227-3.

Abstract

Increasing demand for fire safety has aroused the enthusiasm of researchers for exploring early-stage fire-warning materials. Herein, an early-stage fire-warning cotton fabric (denoted as CF-CP-FR) was designed with a two-layered structure: conducting polymer layer and flame-retardant layer, through *in-situ* chemical oxidation polymerization of polypyrrole (PPy) and dip coating of the compound of montmorillonite and ammonium polyphosphate (MMT@APP), respectively. Based on the thermoelectric effect of the PPy, CF-CP-FR was endowed with accurate temperature sensing capability below 100°C. When encountering fire, CF-CP-FR showed excellent fire-warning response as fast as 1.0 s and displayed repeatable fire-warning capability under the protection of the MMT@APP. Via the mechanism of thermo-induced resistance change, the coated cotton fabric could also trigger the fire warning circuit at ca. 2.0 s. Meanwhile, the flame retardancy and thermal stability of CF-CP-FR were significantly enhanced, owing to the synergetic effect of MMT and APP. This work is promising in fabricating multifunctional clothing with efficient fire safety and smart fire-warning capability.

Introduction

In 2021, fire disasters lead to 3,800 civilian fire deaths and nearly $15.9 billion loss in the US (Shelby and Ben 2022). Therefore, studying how to minimize the damage caused by fire accidents is essential. Extensive research has proved that the involvement of flame-retardant (FR) materials or technologies could effectively protect human lives and property in a fire accident (Lazar et al. 2020; Liu et al. 2021).

Flame retardant material can suppress flame spread and reduce hazardous combustion. However, the sole usage of flame-retardant material is not able to warn humans of the occurrence of fire accidents in time, so the individuals involved hardly can instantly take effective measures to escape or extinguish the fire. Hence, detecting the fire by monitoring chemical or physical signals could earn people more time to react.

Traditional fire-warning material works by detecting smoke or heat. Whereas, this fire-warning material responds slowly (> 100s), and the distance between the smoke and the fire-warning material determines the time of response (Li et al. 2022a; Lv et al. 2022). Hence, developing early-stage fire-warning materials capable of fast fire detection is crucial and meaningful.

Early-stage fire-warning material could respond to temperature intelligently, generating physical or chemical changes, such as the variation in shape (Jia et al. 2022)/phase (Zhao et al. 2021), color (Fu et al. 2019), or electrical conductivity, thermoelectric effect (TE), or gaseous products, etc. Nowadays, MXene, two-dimensional (2D) transition-metal carbides and/or nitride, and graphene oxide (GO) are frequently used for early-stage fire warning (He et al. 2022). Under the attack of flame, the electrical resistance of GO decreases through a thermal-induced reduction process, inducing the fire-warning signal (Wei et al. 2022). Tang et al. explored a lot in GO-based fire-warning material (Guo et al. 2020a; Huang et al. 2020; Yu et al. 2021; Zhang et al. 2020). The fire warning speed was remarkably enhanced, and the

corresponding trigger time could be within 1.0 s (Cao et al. 2022a; Cao et al. 2022b). For TE-based fire-warning material, thermoelectric voltage is sensitive to temperature, and it could be monitored to trigger a fire-warning signal. Zeng et al. carried out many works on MXene-based fire-warning material (Jiang et al. 2022; Wang et al. 2021; Zeng et al. 2022). Notably, this TE-based fire-warning response could be repeatable, which is meaningful for releasing multiple alarm signals. However, these works only focus on the mechanism of thermo-induced resistance transition, and there is no report on the fire warning material capable of working via dual mechanisms (including thermoelectric effect and electrical resistance dependence on temperature).

Polypyrrole (PPy) is a traditional conducting polymer composed of pyrrole rings connected to each other at the 2- and 5-postions, and it could be prepared by chemical oxidation or electrochemical polymerization. Benefiting from the merits of low thermal conductivity, relatively easy processing, environmental stability, low toxicity, etc., polypyrrole is widely applied in biomedical, electrical, and thermoelectrical areas (Nezakati et al. 2018; Yao et al. 2019). Researchers have studied how to enhance the performance of PPy as a thermoelectrical material or device (Maddison et al. 1988; Wang et al. 2014a; Xu et al. 2021), but it is not further applied in the early-stage fire warning. The electrical conductivity of PPy is sensitive to temperature, known as the electrical conductivity dependent on temperature for semiconductors (Le et al. 2017), which may be promising in the area of thermo-induced resistance-type fire-warning material.

Herein, a smart fire-warning cotton fabric was fabricated with *in-situ* polymerized PPy as a fire-warning layer and montmorillonite (MMT) @ ammonium polyphosphate (APP) as a flame-retardant layer, which could be utilized for the early-stage fire warning via a dual mechanism, including the TE effect and thermo-induced resistance change. Based on the TE effect of PPy, the composite cotton fabric showed accurate temperature-sensing capability below 100°C, and it could trigger the alarm lamp in 1.0 s. Notably, this fire warning response is repeatable till the burnout of the coated fabric. In addition, it could successfully give out a warning signal based on the temperature dependence of the resistance of PPy. Fire-warning performance was investigated by a fire-warning test and by detecting the relationship between the output voltage and temperature. The flame retardancy and thermal stability were studied through the vertical burning test (VBT) and thermogravimetric analysis (TGA). The morphology of the obtained cotton fabrics was studied by scanning electron microscopy (SEM).

Experimental

Materials

Ethanol anhydrous (EtOH, ≥ 99.7%) was supplied by Tianjin Zhiyuan Chemical Reagent Co., Ltd (Tianjin, China). Deionized (DI) water and Hydrochloric acid (HCl, 37 wt%) were purchased from Guangzhou Chemical Reagent Factory (Guangzhou, China). Pyrrole (Py, analytical pure grade) and iron chloride ($FeCl_3$, chemical pure grade) were purchased from Shanghai Macklin Biochemical Co., Ltd. (Shanghai, China). Sodium montmorillonite (MMT) and ammonium polyphosphate (APP, degree of polymerization >

1000) were provided by Minerals Technologies Inc. (New York, USA) and JLS Chemical Inc. (Hangzhou, China), respectively. The above reagents were used directly without further purification. Cotton fabric (CF) without any flame-retardant components was obtained from Guangdong Demei Fine Chemical Co., Ltd (Foshan, China).

Preparation of PPy-coated cotton fabric (CF-CP)

CF was separately washed with deionized water and ethanol alternately to remove possible impurities, which was followed by being dried in an oven at 60°C for 1h. Then, it was immersed in an ethanol solution of pyrrole (10 vol%) for 5 mins, which was transferred into a mixed solution of $FeCl_3$ and HCl (the molar ratio of $FeCl_3$/HCl is 0.31/0.3) for 15 mins. After being dried in an oven at 60°C for 1h, the conducting polymer layer was successfully prepared. The above processes were carried out several times, and the obtained coated CF was noted as CF-CP_X, where X represented the times of polymerization, ranging from 1 to 6.

Construction of MMT@APP-coated CF-CP (CF-CP-FR)

MMT and APP with a mass ratio of 1.2/5 were added into DI water for stirring overnight to form a universally dispersed suspension (7.3 wt%), which was marked as MMT@APP. Through dip coating, MMT@APP was coated onto CF-CP_X. Subsequently, it was hung vertically in an oven at 60°C for 1h. This process was performed multiple times, and the treated CF-CP_X was noted as CF-CP_X-FR_Y, where Y represented the weight increment percentage of MMT@APP. The compositions of all coated samples are listed in Table 1.

Table 1
Weight increment of the coated cotton fabric

Sample	Pure mass loading of each component	
	PPy (wt %)	MMT@APP (wt %)
CF-CP_1-$FR_{80\%}$	5.6	~ 80%
CF-CP_2-$FR_{80\%}$	13.5	
CF-CP_3-$FR_{80\%}$	21.9	
CF-CP_4-$FR_{80\%}$	31.3	
CF-CP_5-$FR_{80\%}$	45.1	
CF-CP_6	51.5	-
CF-CP_6-$FR_{30\%}$		~ 30%
CF-CP_6-$FR_{80\%}$		~ 80%

Characterization

Thermogravimetric analysis (TGA)

Thermal stability was studied by a thermogravimetric analyzer (TG209 F3, Netzsch, Germany) at a heat rate of 20°C/min under a nitrogen atmosphere with a flow of 40 mL/min. All samples were scanned over a temperature range from 25°C to 900°C.

Vertical burning test (VBT)

Vertical burning tests were carried out in a flame cabinet according to ASTM D6413-08. The control and coated samples with a size of 100mm*45mm were exposed to a direct flame from an alcohol lamp for 12 s.

Scanning electron microscopy (SEM)

The morphology and microstructure of all samples before and after the VBT test were characterized by scanning electron microscopy (SU8220, Hitachi, Japan) at an accelerating voltage of 5 kV. The samples were sputter coated with a thin layer of Au/Pd prior to SEM imaging.

Temperature sensing test

The CF-CP_X-FR_Y was tailored to 70mm*15mm, and one end was placed on a heating platform (JF956B, Jinfeng, China). Then it was connected to a data acquisition/switch unit (34972A, Keysight, US), which could simultaneously monitor the TE voltage and temperature of both sides. The temperature of the heating platform was raised in steps (50, 60, 70, 80, 90, 100, 120, 140, 160, 180, and 200°C). The infrared thermal images were recorded by an Infrared thermal imaging instrument (H10, Hikvision, China).

Fire warning test

For TE effect-based fire-warning test, the control and coated samples with the size of 70mm*15mm were connected with a digital multimeter (UT61E+, 4½, Unit, China) to obtain the real-time TE voltage curve. Simultaneously, the output TE voltage was monitored by a 4½ digital panel meter (SP42DV1, Shenlan, China). When TE voltage exceeded the upper limit (5 mV), the DC voltmeter would make the series circuit composed of a warning lamp and a DC power connected, working as a relay. Real-time voltage was recorded and the trigger time was read from the video capture of the fire-warning test process.

For the thermo-induced resistance change-based fire warning test, the coated samples were connected in series with the DC power and warning lamp. Under a fixed supply voltage, the temperature of the directly heated area and the corresponding current of samples with different cross-section widths during the fire attack were recorded by Keysight 34972A to obtain more details.

Results And Discussion

Preparation and structure of CF-CP-FR

As shown in Fig. 1, the preparation and structure of the CP layer and FR layer are exhibited. Pyrrole was polymerized on the CF fibers by an *in-situ* chemical oxidation polymerization approach. Ferric ions acted as an oxidant, taking an electron from nitrogen in the pyrrole ring and forming a free radical cation, which was the key to dimmer formation and chain propagation (Zare et al. 2021). Meanwhile, chlorine ion was doped into PPy chains along with the chemical oxidation polymerization (Scaccabarozzi et al. 2022). Then PPy-coated CF was dip-coated with MMT@APP, which would function as a flame retardant (FR) layer. Eventually, cotton fabric coated with a double-layer structure was fabricated, which was noted as CF-CP-FR.

Fire-warning performance

Thermoelectric effect-based temperature sensing and fire warning performance

The state-of-art TE-type fire-warning materials are based on the Seebeck effect. Hence, to explore the performance of TE-type fire-warning material, it is necessary to study the Seebeck effect. The Seebeck effect specifies that the temperature difference ($\triangle T$) generated at both ends of thermoelectric materials drives the charge carrier from the hot side to the cold one. Subsequently, the potential difference ($\triangle V$) is formed (Nandihalli et al. 2020). The real-time temperature and thermoelectric voltage (V_{TE}) were detected to calculate the observed Seebeck coefficient (S_{ob}), which can be expressed as Eq. (1) (Park et al. 2018).

$$S_{ob}=-\frac{V_{TE}}{(T_h-T_c)}$$

1

Where T_h and T_c represent the temperature of the hot side and the cold one, respectively.

Figure 2(a) shows the output V_{TE} of CF-CP_3-$FR_{80\%}$ during stepwise heating ranging from 50–200°C, and an evidential linear relationship between V_{TE} and T_h is visible. In addition, there is a rise of V_{TE} at ca. 180°C, revealing a jump of S_{ob}. It is probably due to the degradation of the dopant. Because the Seebeck coefficient tends to increase with the decreased doping level (Wang et al. 2019). As shown in Fig. 2(b), V_{TE} showed a linear relationship with T_h (ranging from 50 to 100°C), fitting the linear equation "V_{TE}=0.01075*T-0.29729". It is consistent with the experimental result that the Seebeck coefficient of PPy almost kept unchanged below 100°C (Wang et al. 2017). Repeated tests confirmed that the linear relationship between V_{TE} and T_h is stable below 100°C. Though the temperature of fire accidents is much higher than 100°C, the S_{ob} obtained below 100°C is still expected to provide insight into exploring the influence factors of the fire-warning speed.

As shown in Fig. 2(c), three sample stripes with the same formula were detected simultaneously, and the infrared thermal image exhibited that the T_c was stable even though the T_h reached 100°C. As shown in Fig. 2(d), T_c remained stable, indicating low thermal conductivity of the coated cotton fabric. Figure 2(e) and Fig. 2 (f) show the V_{TE}-T_h curve and the S_{ob} of all samples, respectively. For CF-CP_1-$FR_{80\%}$, CF-CP_2-$FR_{80\%}$, CF-CP_3-$FR_{80\%,}$ and CF-CP_4-$FR_{80\%}$, the linear least-squares fitting of the data shows that the Seebeck coefficient remains in the range of 10.2 to 10.9 μV/K. With more pick-up of PPy, the Seebeck coefficient starts to decline to the range of 6.3–7.8 μV/K. For CF-CP_1-$FR_{80\%}$ ~ CF-CP_4-$FR_{80\%}$, the discontinuous distribution of PPy particles might probably lead to a limited concentration of effective carriers. Denser PPy coated on CF-CP_5-$FR_{80\%}$ and CF-CP_6-$FR_{80\%}$ provides more effective conductive pathways and a higher level of carrier concentration because there is less interspace.

Thanks to the rise of V_{TE} due to the Seebeck effect, the potential fire risk can be alarmed by constructing a circuit, which is sensitive to the change of V_{TE}. Fire-warning tests were carried out to explore the trigger time and repeatable fire-warning capability of the coated cotton fabric.

In Fig. 3(a), the infrared thermal image snapshots indicated that the temperature of the directly heated area was over 350°C, which was beyond the decomposition temperature of PPy (Wang et al. 2014b). Figure 3(b) shows the trigger time of all the coated samples. For CF-CP_1-$FR_{80\%}$ ~ CF-CP_4-$FR_{80\%}$, the trigger time stayed in the range of 1.5–1.7 s, while 2.9 s and 3.2 s for CF-CP_5-$FR_{80\%}$ and CF-CP_6-$FR_{80\%}$, respectively. The detected trigger time is probably affected by the Seebeck coefficient and the electrical conductivity. While the Seebeck coefficient and the electrical conductivity are interdependent (Ouyang et al. 2019). Hence, the fastest fire-warning response from CF-CP_2-$FR_{80\%}$ may be a comprehensive result of the Seebeck coefficient and the electrical conductivity (Shi et al. 2020).

For early-stage fire-warning material, the repeatable fire-warning capability is meaningful for releasing the fire-warning signal multiple times. In Fig. 4 (a), the repeatable fire-warning capability of the coated fabric was verified. When the fire approached CF-CP2-FR80%, a rapid rise in the VTE was observed, and the fire-warning lamp was triggered at the same time. The warning lamp was triggered again after nearly 1min without removing the fire. The secondary fire alarm lasted nearly 30 s till the fire was removed, as shown in the video 1 (Online resource 1). As shown in Fig. 4 (b), the sample could withstand a 5-minute fire attack and give rise to multi-time fire-warning signals until it was burned out. The video snapshots of CF-CP2-FR80% also revealed that the first fire warning signal was the fastest. Beyond that, the output VTE of the rest fire-warning responses was smaller than the first one, which was probably due to the decreased amount of PPy retained on the hot side.

Thermo-induced resistance change-based fire warning performance

It is more convenient to construct a fire-warning circuit of resistance-type fire-warning material than that of TE-type. Research on resistance-type fire-warning material provides a facile and meaningful strategy to

earn individuals more time for evacuation. Whereas, there is no report on exploring PPy as a resistance-type fire-warning material. In this section, the thermo-induced resistance change-based response of the obtained material was studied.

Notably, the obtained CF-CP-FR also showed the potential as a resistance-type fire warning material. For PPy, the temperature dependence of the electrical conductivity can be utilized for fire warning. As shown in Fig. 5, the fire warning lamp could be triggered at around 2s, though the light was faint. When the CF-CP-FR was exposed to the flame, the trend of current rising is consistent with the well-known temperature dependence on electrical conductivity for semiconductors (Kaiser 2001; Taunk et al. 2010).

Meanwhile, experimental results revealed that the cross-section width of the coated cotton fabric affected the real-time current, as shown in Fig. 6. When the sample was exposed to flame, the corresponding temperature rapidly raised and the electrical resistance decreased, inducing the rise in current. At around 8s, the current of both samples reached the maximum. After that, the current declined because the decomposition of PPy underwent simultaneously. Compared with the sample with a 1.5 cm wide cross-section, CF-CP_3-$FR_{80\%}$ with a 3.0 cm wide cross-section displayed a climb in the current again, which reached a secondary peak after ca. 1 min. Because conductive pathways were not destructed completely during the fire attack, the current could rise again when the heat was transferred to the area nearby. This finding demonstrates the cross-section size of the sample could affect the thermo-induced resistance change-based fire-warning response.

Flame retardancy and thermal stability

VBT test was conducted to study the flame retardancy of the control and coated cotton fabrics. As shown in Fig. 7 (a), CF was ignited immediately and burned out completely. Under the protection of the FR layer, the flame retardancy of CF-$FR_{80\%}$ was significantly improved and the flame was suppressed. Our previous research has proved that the cooperation of MMT and APP can produce a dense char and generate a synergetic flame-retardant effect (Zhang et al. 2021; Zhang et al. 2017). However, without PPy coating, CF and CF-$FR_{80\%}$ were not sensitive to flame attack, as shown in the video 2 and 3 (Online resource 1). Compared with pristine CF, CF-CP_6 exhibited improved flame retardancy, but it was insufficient to suppress the flame. Meanwhile, CF-CP_6 exhibited a rapid rise in V_{TE}, but the V_{TE} dropped immediately and the whole fabric was burned out. Hence, as shown in the video 4 (Online resource 1). The cotton fabric only coated with PPy can release a transient thermoelectric voltage signal, but the limited flame retardancy cannot guarantee repeatable fire-warning capability. Among these four samples, CF-CP_6-$FR_{80\%}$ can not only achieve flame retardancy but also demonstrate the capability of repeatable fire-warning capability.

TG test was carried out to further investigate the thermal stability of the samples in a nitrogen atmosphere. As shown in Fig. 7 (b), all samples exhibited a small weight loss at approximately 100°C, which might originate from the absorbed water (Wang et al. 2014a). With the temperature increasing, the samples coated with the CP layer exhibited another tiny weight loss starting at ca.160°C, which might be

the removal of the counter anions (Hebeish et al. 2016; Varesano et al. 2008). For CF, the main weight loss underwent approximately ranging from 300°C to 410°C due to the degradation of cellulose, including de-polymerization, dehydration, and decomposition of glycosyl (Guo et al. 2020b; Poletto et al. 2014). The temperature at maximum mass loss rate (T_{max}) was ca. 375°C, leaving 8.8% char residue at 900°C. For CF-FR, it displayed a tiny mass loss rate at ca. 240°C, which is related to the production of phosphoric acid and NH_3 through the decomposition of APP. Then, the phosphoric acid catalyzed the dehydration of PPy, promoting the formation of a dense char layer with the help of MMT (He et al. 2016). This is why all samples coated with MMT@APP exhibited an earlier onset degradation temperature. In addition, the char yield at 900°C of CF-FR was 45.2%. According to the above analysis, the effective flame retardancy of MMT@APP was verified. T_{max} of the samples coated with PPy was reduced, owing to the earlier degradation of PPy at ca. 260°C (Wu et al. 2014). Moreover, the maximum mass loss rate of the samples coated with PPy was smaller than the control CF. This is probably related to the char formation effect of PPy, owing to the rich content of nitrogen (Abu Elella et al. 2021; Attia 2017; Attia et al. 2015; Goda et al. 2021). Notably, the char residuals at 900°C of CF-CP_6-$FR_{30\%}$ and CF-CP_6-$FR_{80\%}$ were enhanced to 40.0% and 45.2%, respectively. Meanwhile, the maximum mass loss rate that occurred at ca. 340°C was reduced, indicating a better flame retardancy could be endowed with the increment of MMT@APP. In all, with the synergistic effect of MMT and APP, the flame retardancy and thermal stability of CF-CP_6-$FR_{80\%}$ were considerably improved.

Morphology and microstructure

SEM was employed to study the morphology and microstructure of the control and treated cotton fabrics, as exhibited in Fig. 8. Before VBT, the cotton fiber surface was smooth, as shown in Fig. 8 (a). In Fig. 8 (b), PPy particles clustered closely on the surface of cotton fibers. Figure 8 (c) showed the packing of layered micro-size particles, which was the compound of MMT and APP. The layer structure indicated that MMT nanosheets were exfoliated by APP.

After VBT, the control cotton fiber collapsed apparently, and the surface became relatively coarse. For CF-CP_6, a host of PPy spherical particles were destructed, forming large number of voids. The morphology of CF-$FR_{80\%}$ was the same as that of CF-CP_6-$FR_{80\%}$, so it is not presented here. For CF-CP_6-$FR80_{\%}$, the shape of micro-sized MMT@APP particles changed from a cuboid to a dense bubble-like char layer, which could effectively hinder heat transition and oxygen diffusion. The above SEM results are consistent with the TG and VBT results, approving the flame retardancy of the samples coated with MMT@APP.

Flame-retardant and fire-warning mechanism

MMT@APP and *in-situ* polymerized PPy were designed to endow cotton fabrics with excellent flame retardancy and fire-waring performance, and the corresponding mechanisms are discussed herein.

When the temperature increased, a dense char was formed thanks to the synergetic effect of MMT and APP. This char layer could protect the PPy layer and substrate from being destructed by the fire.

Therefore, this flame-retardant layer not only endowed the obtained material with fire-safety capability but also played a key role in guaranteeing the repeatable fire-warning capability.

Under the protection of MMT@APP, *in-situ* synthesized PPy could trigger the fire-warning signal repeatedly when encountering flame, functioning in the mechanism of thermoelectric effect. As shown in Fig. 9 (a), holes in the PPy layer were activated by heat and migrated following the temperature difference along the PPy chains. With the accumulation of positive charges on the cold side, the thermoelectric potential difference was set up extremely fast, which could be built up repeatedly. Hence, the thermoelectric fire-warning response could be rapid and repeatable.

Figure 9 (b) shows the circuit of thermo-induced resistance change-based response for fire warning. Generally, the conductivity of conducting polymers (including polypyrrole, polyaniline, polythiophene, etc.) increases with rising temperature. Hence, under fire attack, the current in the circuit climbed corresponding to the decreasing electrical resistance of PPy, and this characteristic endowed the obtained material with thermo-induced resistance change-based fire-warning capability.

The fie-waning performance between CF-CP-FR in this work and other state-of-art fire-warning materials is compared, which is concluded in Table 2. For thermoelectric-mechanism material, this work exhibited an outstanding fire-warning speed (1.0 s), and the repeatable fire-waring capability was also achieved. Meanwhile, there are no publications about the thermo-induced resistance response of PPy for fire warning, which was explored in this work. The trigger time of the thermo-induced resistance change-based fire warning could reach 2 s. There still exists room for exploring repeatable fire-warning capability and improving the fire-warning speed, but our work may inspire those researchers who are interested in thermo-induced resistance change-based fire warning of PPy.

Table 2
Comparison of the fie-waning performance between CF-CP-FR in this work and other fire-warning materials.

Composition*	Trigger time (s)	Thermoelectric response	Thermo-induced resistance change-based response	Ref
MXene/UPC/MMT	3.1	Yes	-	(Zeng et al. 2022)
MXene/ polyimide	> 2	Yes	-	(Jiang et al. 2022)
MXene/CCS@CF	~ 3.8	Yes	-	(Wang et al. 2021)
CF/CB@KF/CNT/PVA	4	-	Yes	(Xia et al. 2022)
PA@MGO paper	2	-	Yes	(Li et al. 2022b)
PAN/CNTs/APP fiber	5	-	Yes	(Zhao et al. 2022)
GO-BA paper	0.5	-	Yes	(Yuan et al. 2021)
PPy/MMT@APP-CF	**1.0 (~ 2.0)**	**Yes**	**(Yes)**	**This work**

*: MFNC, multifunctional fire protection nanocoating; UPC, 2-ureido-4[1H]-pyrimidinone-containing cellulose; MMT, montmorillonite; CCS, carboxymethyl chitosan; CF, cotton fabric; CB@KF, carbon black nanoparticles with core-shell structure; CNT, carbon nanotube; PVA, poly (vinyl alcohol); PA, phytic acid; MGO; compound of MXene and GO; GO, graphene oxide; PAN, polyacrylonitrile; APP, ammonium polyphosphate; BA, boric acid.

Conclusion

Early-stage fire-warning cotton fabric was successfully prepared by *in-situ* polymerization of PPy and dip coating of MMT@APP. The cotton fabric was endowed with excellent flame retardancy due to the synergistic effect of MMT and APP. More importantly, the flame-retardant layer could protect the thermoelectric layer from being damaged by the flame and ensure the repeatable fire warning capability of CF-CP-FR. Thanks to the thermoelectric effect of PPy and the protection from MMT@APP, the obtained cotton fabric showed accurate temperature sensing capability below 100°C, and it could trigger the fire warning circuit as fast as 1.0 s. Significantly, it exhibited repeatable fire-warning capability. Meanwhile, the coated cotton fabric could also trigger the fire warning circuit through a thermo-induced resistance change-based response. This work opens a new sight into the design of fire-warning materials capable of working via a dual mechanism, and is promising in the applications of e-textiles such as functional

clothing with fire protection, temperature sensing, and fire-warning capability. The coating strategy of this work is facile and can be applied to different substrates for various application scenarios.

Declarations

Ethics approval and consent to participate

Not applicable

Consent for publication

Not applicable

Availability of data and materials

Supporting information has been uploaded as video materials.

Competing interests

The authors declare that we do not have any conflict of interest in the submission of this manuscript.

Funding

This work is financially supported by National Natural Science Foundation of China (21878114), Natural Science Foundation of Guangdong Province of China (2021A1515010289) and Guangzhou Science and Technology Program 202201020231 . This research is also supported by the Opening Project of Key Laboratory of Polymer Processing Engineering (KFKT2005, South China University of Technology), Ministry of Education.

Author contributions

Tao Zou: Conceptualization, Methodology, Investigation, Formal Analysis, Data Curation, Visualization, Writing - Original Draft;

Dongqiao Zhang (corresponding author): Conceptualization, Methodology, Supervision, Writing- Review & Editing

Tao Xu (corresponding author): Supervision, Writing-Review & Editing;

Xiaohong Peng: Supervision, Writing-Review & Editing

He Zhang: Writing -Review & Editing

Yanliang Du: Writing -Review & Editino

Acknowledgements

The authors would like to acknowledge the financial support of National Natural Science Foundation of China (21878114), Natural Science Foundation of Guangdong Province of China (2021A1515010289) and Guangzhou Science and Technology Program 202201020231 . This research is also supported by the Opening Project of Key Laboratory of Polymer Processing Engineering (KFKT2005, South China University of Technology), Ministry of Education.

References

1. Shelby H, Ben E. Fire Loss in the United States During 2021 [R].National Fire Protection Association (NFPA). 2022.
2. Lazar ST, Kolibaba TJ, Grunlan JC (2020) Flame-retardant surface treatments. Nature Reviews Materials 5:259-275. https://doi.org/https://doi.org/10.1038/s41578-019-0164-6
3. Liu BW, Zhao HB, Wang YZ (2021) Advanced Flame-Retardant Methods for Polymeric Materials. Advanced Materials:2107905-21079341. https://doi.org/https://doi.org/10.1002/adma.202107905
4. Li X, Vazquez-Lopez A, Sanchez Del Rio Saeza J et al. (2022a) Recent Advances on Early-Stage Fire-Warning Systems: Mechanism, Performance, and Perspective. Nano-Micro Letters 14:197-229. https://doi.org/https://doi.org/10.1007/s40820-022-00938-x
5. Lv L-Y, Cao C-F, Qu Y-X et al. (2022) Smart fire-warning materials and sensors: Design principle, performances, and applications. Materials Science and Engineering: R: Reports 150:100690-1006731. https://doi.org/https://doi.org/10.1016/j.mser.2022.100690
6. Jia J, Gao N, Li R et al. (2022) An "OFF-to-ON" shape memory polymer conductor for early fire disaster alarming. Chemical Engineering Journal 431:133285-133295. https://doi.org/https://doi.org/10.1016/j.cej.2021.133285
7. Zhao X, Peng L-M, Chen Y et al. (2021) Phase change mediated mechanically transformative dynamic gel for intelligent control of versatile devices. Materials Horizons 8:1230-1241. https://doi.org/https://doi.org/10.1039/d0mh02069a
8. Fu T, Zhao X, Chen L et al. (2019) Bioinspired Color Changing Molecular Sensor toward Early Fire Detection Based on Transformation of Phthalonitrile to Phthalocyanine. Advanced Functional Materials 29:1806586-1806594. https://doi.org/https://doi.org/10.1002/adfm.201806586
9. He X, Feng Y, Xu F et al. (2022) Smart fire alarm systems for rapid early fire warning: Advances and challenges. Chemical Engineering Journal 450:137927-137950. https://doi.org/https://doi.org/10.1016/j.cej.2022.137927
10. Wei W, Yi Y, Song J et al. (2022) Tunable Graphene/Nitrocellulose Temperature Alarm Sensors. Acs Applied Materials & Interfaces 14:13790-13800. https://doi.org/https://doi.org/10.1021/acsami.2c02340
11. Guo K-Y, Wu Q, Mao M et al. (2020a) Water-based hybrid coatings toward mechanically flexible, super-hydrophobic and flame-retardant polyurethane foam nanocomposites with high-efficiency and

reliable fire alarm response. Composites Part B: Engineering 193:108017-108028. https://doi.org/https://doi.org/10.1016/j.compositesb.2020.108017

12. Huang N-J, Xia Q-Q, Zhang Z-H et al. (2020) Simultaneous improvements in fire resistance and alarm response of GO paper via one-step 3-mercaptopropyltrimethoxysilane functionalization for efficient fire safety and prevention. Composites Part A: Applied Science and Manufacturing 131:105797-105807. https://doi.org/https://doi.org/10.1016/j.compositesa.2020.105797
13. Yu Z-R, Mao M, Li S-N et al. (2021) Facile and green synthesis of mechanically flexible and flame-retardant clay/graphene oxide nanoribbon interconnected networks for fire safety and prevention. Chemical Engineering Journal 405:126620-126632. https://doi.org/https://doi.org/10.1016/j.cej.2020.126620
14. Zhang ZH, Zhang JW, Cao CF et al. (2020) Temperature-responsive resistance sensitivity controlled by L-ascorbic acid and silane co-functionalization in flame-retardant GO network for efficient fire early-warning response. Chemical Engineering Journal 386:123894-123904. https://doi.org/https://doi.org/10.1016/j.cej.2019.123894
15. Cao CF, Yu B, Chen ZY et al. (2022a) Fire Intumescent, High-Temperature Resistant, Mechanically Flexible Graphene Oxide Network for Exceptional Fire Shielding and Ultra-Fast Fire Warning. Nano-Micro Letters 14:1-18. https://doi.org/https://doi.org/10.1007/s40820-022-00837-1
16. Cao CF, Yu B, Guo BF et al. (2022b) Bio-inspired, sustainable and mechanically robust graphene oxide-based hybrid networks for efficient fire protection and warning. Chemical Engineering Journal 439:134516-134520. https://doi.org/https://doi.org/10.1016/j.cej.2022.134516
17. Jiang C, Chen J, Lai X et al. (2022) Mechanically robust and multifunctional polyimide/MXene composite aerogel for smart fire protection. Chemical Engineering Journal 434:134630-134639. https://doi.org/https://doi.org/10.1016/j.cej.2022.134630
18. Wang B, Lai X, Li H et al. (2021) Multifunctional MXene/Chitosan-Coated Cotton Fabric for Intelligent Fire Protection. Acs Applied Materials & Interfaces 13:23020-23029. https://doi.org/https://doi.org/10.1021/acsami.1c05222
19. Zeng Q, Zhao Y, Lai X et al. (2022) Skin-inspired multifunctional MXene/cellulose nanocoating for smart and efficient fire protection. Chemical Engineering Journal 446:136899-136909. https://doi.org/https://doi.org/10.1016/j.cej.2022.136899
20. Nezakati T, Seifalian A, Tan A et al. (2018) Conductive Polymers: Opportunities and Challenges in Biomedical Applications. Chemical Reviews 118:6766-6843. https://doi.org/https://doi.org/10.1021/acs.chemrev.6b00275
21. Yao CJ, Zhang HL, Zhang Q (2019) Recent Progress in Thermoelectric Materials Based on Conjugated Polymers. Polymers 11:107-126. https://doi.org/https://doi.org/10.3390/polym11010107
22. Maddison DS, Unsworth J, Roberts RB (1988) Electrical conductivity and thermoelectric power of polypyrrole with different doping levels. Synthetic Metals 26:99-108. https://doi.org/https://doi.org/10.1016/0379-6779(88)90339-6

23. Wang L, Liu F, Jin C et al. (2014a) Preparation of polypyrrole/graphene nanosheets composites with enhanced thermoelectric properties. RSC Advances 4:46187-46193. https://doi.org/https://doi.org/10.1039/c4ra07774a
24. Xu S, Shi X-L, Dargusch M et al. (2021) Conducting polymer-based flexible thermoelectric materials and devices: From mechanisms to applications. Progress in Materials Science 121:100840-100906. https://doi.org/https://doi.org/10.1016/j.pmatsci.2021.100840
25. Le TH, Kim Y, Yoon H (2017) Electrical and Electrochemical Properties of Conducting Polymers. Polymers 9:150-182. https://doi.org/https://doi.org/10.3390/polym9040150
26. Zare EN, Agarwal T, Zarepour A et al. (2021) Electroconductive multi-functional polypyrrole composites for biomedical applications. Applied Materials Today 24:101117-101152. https://doi.org/https://doi.org/10.1016/j.apmt.2021.101117
27. Scaccabarozzi AD, Basu A, Anies F et al. (2022) Doping Approaches for Organic Semiconductors. Chemical Reviews 122:4420-4492. https://doi.org/https://doi.org/10.1021/acs.chemrev.1c00581
28. Nandihalli N, Liu C-J, Mori T (2020) Polymer based thermoelectric nanocomposite materials and devices: Fabrication and characteristics. Nano Energy 78:105186-105205. https://doi.org/https://doi.org/10.1016/j.nanoen.2020.105186
29. Park H, Kim JW, Hong SY et al. (2018) Microporous Polypyrrole-Coated Graphene Foam for High-Performance Multifunctional Sensors and Flexible Supercapacitors. Advanced Functional Materials 28:1707013-1707024. https://doi.org/https://doi.org/10.1002/adfm.201707013
30. Wang Y, Yang L, Shi XL et al. (2019) Flexible Thermoelectric Materials and Generators: Challenges and Innovations. Advanced Materials 31:1807916-1180763. https://doi.org/https://doi.org/10.1002/adma.201807916
31. Wang YH, Yang J, Wang LY et al. (2017) Polypyrrole/Graphene/Polyaniline Ternary Nanocomposite with High Thermoelectric Power Factor. Acs Applied Materials & Interfaces 9:20124-20131. https://doi.org/https://doi.org/10.1021/acsami.7b05357
32. Wang J, Cai KF, Shen S et al. (2014b) Preparation and thermoelectric properties of multi-walled carbon nanotubes/polypyrrole composites. Synthetic Metals 195:132-136. https://doi.org/https://doi.org/10.1016/j.synthmet.2014.06.003
33. Ouyang Y, Zhang Z, Li D et al. (2019) Emerging Theory, Materials, and Screening Methods: New Opportunities for Promoting Thermoelectric Performance. Annalen der Physik 531:1800437-1800463. https://doi.org/https://doi.org/10.1002/andp.201800437
34. Shi XL, Zou J, Chen ZG (2020) Advanced Thermoelectric Design: From Materials and Structures to Devices. Chemical Reviews 120:7399-7515. https://doi.org/https://doi.org/10.1021/acs.chemrev.0c00026
35. Kaiser AB (2001) Systematic conductivity behavior in conducting polymers: Effects of heterogeneous disorder. Advanced Materials 13:927-941. https://doi.org/https://doi.org/10.1002/1521-4095(200107)13:12/13<927::Aid-adma927>3.0.Co;2-b

36. Taunk M, Kapil A, Chand S (2010) Chemical synthesis and low temperature electrical transport in polypyrrole doped with sodium bis(2-ethylhexyl) sulfosuccinate. Journal of Materials Science: Materials in Electronics 22:136-142. https://doi.org/https://doi.org/10.1007/s10854-010-0102-2
37. Zhang DQ, Williams BL, Liu JJ et al. (2021) An environmentally-friendly sandwich-like structured nanocoating system for wash durable, flame retardant, and hydrophobic cotton fabrics. Cellulose 28:10277-10289. https://doi.org/https://doi.org/10.1007/s10570-021-04177-y
38. Zhang DQ, Williams BL, Shrestha SB et al. (2017) Flame retardant and hydrophobic coatings on cotton fabrics via sol-gel and self-assembly techniques. Journal of Colloid and Interface Science 505:892-899. https://doi.org/https://doi.org/10.1016/j.jcis.2017.06.087
39. Hebeish A, Farag S, Sharaf S et al. (2016) Advancement in conductive cotton fabrics through in situ polymerization of polypyrrole-nanocellulose composites. Carbohydrate polymers 151:96-102. https://doi.org/https://doi.org/10.1016/j.carbpol.2016.05.054
40. Varesano A, Tonin C, Ferrero F et al. (2008) Thermal stability and flame resistance of polypyrrole-coated PET fibres. Journal of Thermal Analysis and Calorimetry 94:559-565. https://doi.org/https://doi.org/10.1007/s10973-007-8639-x
41. Guo W, Wang X, Huang J et al. (2020b) Construction of durable flame-retardant and robust superhydrophobic coatings on cotton fabrics for water-oil separation application. Chemical Engineering Journal 398:125661-125676. https://doi.org/https://doi.org/10.1016/j.cej.2020.125661
42. Poletto M, Ornaghi HL, Zattera AJ (2014) Native Cellulose: Structure, Characterization and Thermal Properties. Materials 7:6105-6119. https://doi.org/https://doi.org/10.3390/ma7096105
43. He X, Zhang W, Yi D et al. (2016) Flame retardancy of ammonium polyphosphate–montmorillonite nanocompounds on epoxy resin. Journal of Fire Sciences 34:212-225. https://doi.org/https://doi.org/10.1177/0734904116637213
44. Wu J, Sun Y, Pei W-B et al. (2014) Polypyrrole nanotube film for flexible thermoelectric application. Synthetic Metals 196:173-177. https://doi.org/https://doi.org/10.1016/j.synthmet.2014.08.001
45. Abu Elella MH, Goda ES, Yoon KR et al. (2021) Novel vapor polymerization for integrating flame retardant textile with multifunctional properties. Composites Communications 24:100614-100621. https://doi.org/https://doi.org/10.1016/j.coco.2020.100614
46. Attia NF (2017) Organic nanoparticles as promising flame retardant materials for thermoplastic polymers. Journal of Thermal Analysis and Calorimetry 127:2273-2282. https://doi.org/https://doi.org/10.1007/s10973-016-5740-z
47. Attia NF, El Ebissy AA, Hassan MA (2015) Novel synthesis and characterization of conductive and flame retardant textile fabrics. Polymers for Advanced Technologies 26:1551-1557. https://doi.org/https://doi.org/10.1002/pat.3580
48. Goda ES, Abu Elella MH, Hong SE et al. (2021) Smart flame retardant coating containing carboxymethyl chitosan nanoparticles decorated graphene for obtaining multifunctional textiles. Cellulose 28:5087-5105. https://doi.org/https://doi.org/10.1007/s10570-021-03833-7

49. Xia L, Lv Y, Miao Z et al. (2022) A flame retardant fabric nanocoating based on nanocarbon black particles@polymer composite and its fire-alarm application. Chemical Engineering Journal 433:133501-133512. https://doi.org/https://doi.org/10.1016/j.cej.2021.133501
50. Li X, Sánchez del Río Saez J, Ao X et al. (2022b) Highly-sensitive fire alarm system based on cellulose paper with low-temperature response and wireless signal conversion. Chemical Engineering Journal 431:134108-134118. https://doi.org/https://doi.org/10.1016/j.cej.2021.134108
51. Zhao T, Teng D, Xu Y et al. (2022) Multi-functional air filters with excellent flame retardancy and fire-warning capability. Journal of Colloid and Interface Science 617:236-245. https://doi.org/https://doi.org/10.1016/j.jcis.2022.03.003
52. Yuan B, Wang Y, Chen G et al. (2021) Nacre-like graphene oxide paper bonded with boric acid for fire early-warning sensor. Journal of Hazardous Materials 403:123645-123644. https://doi.org/https://doi.org/10.1016/j.jhazmat.2020.123645

Figures

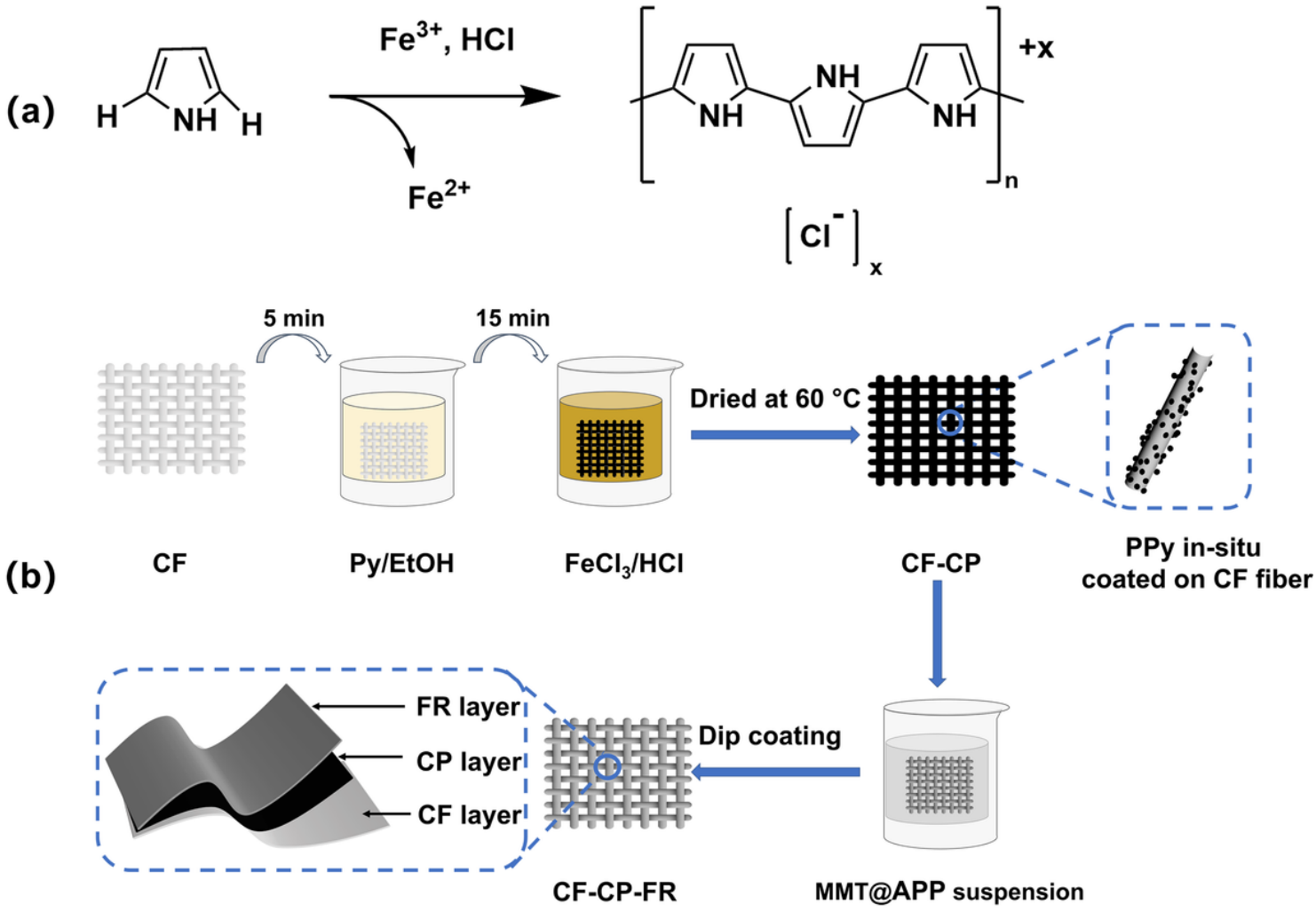

Figure 1

Schematic illustration of the preparation of CF-CP-FR: (a) Chemical oxidation polymerization of pyrrole; (b) fabrication process of the obtained fire-warning material

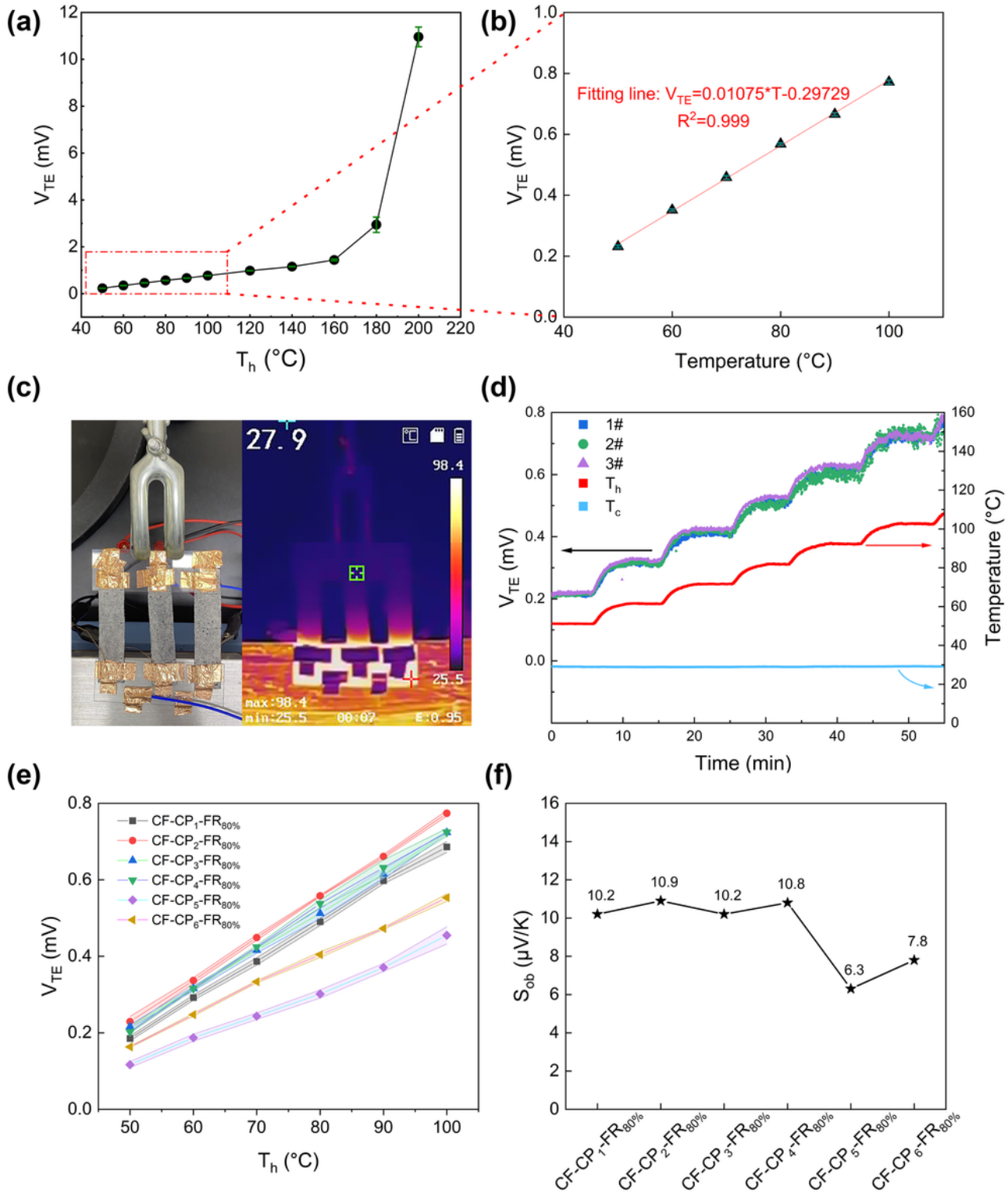

Figure 2

Temperature sensing performance: (a) The output VTE of CF-CP3-FR80% during temperature sensing test; (b) Linear fitting line of V_{TE} vs temperature ranging from 50 °C to 100 °C; (c) Digital and thermal infrared

images of CF-CP_3-$FR_{80\%}$; (d) Real-time V_{TE} and temperature curves during temperature sensing test; (e) V_{TE} vs T_h curves of CF-CP_1-$FR_{80\%}$ ~ CF-CP_4-$FR_{80\%}$; (f) The observed Seebeck coefficient data read from the slope of V_{TE}-T_h curves in Fig. 2(e)

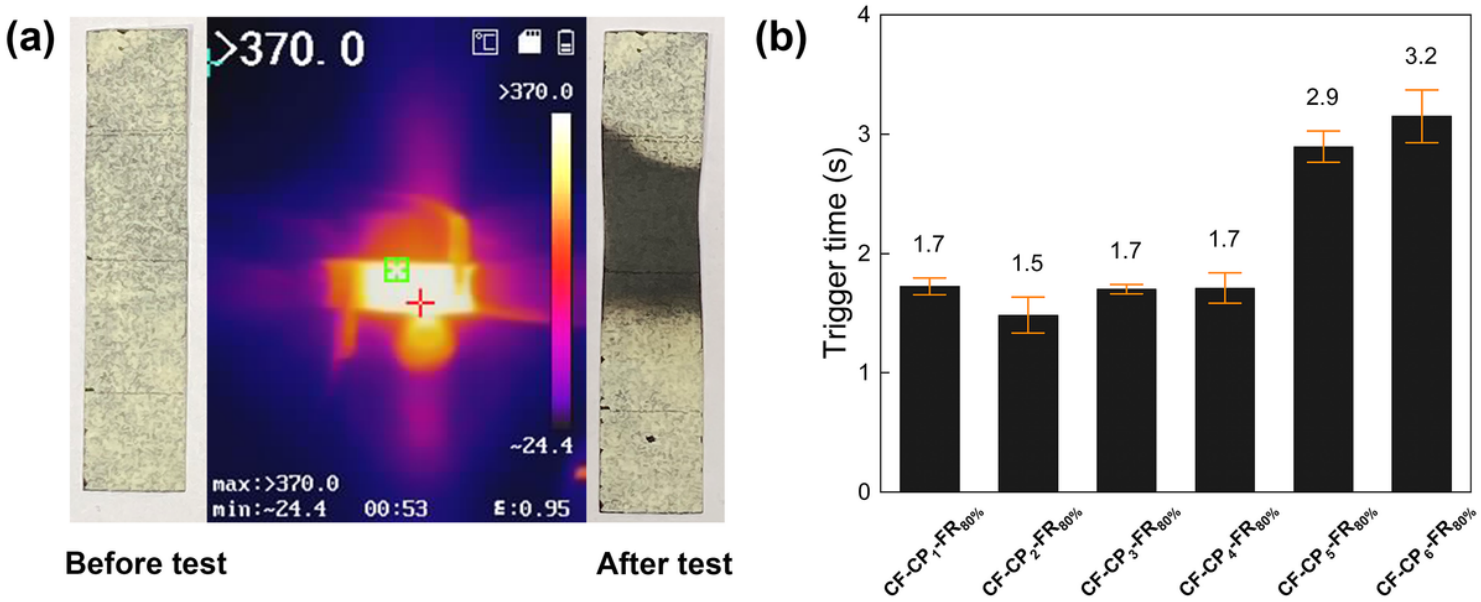

Figure 3

(a) Digital and thermal imaging picture of CF-CP_2-$FR_{80\%}$ before, during, and after the fire-warning test, (b) The trigger time of CF-CP_1-$FR_{80\%}$~ CF-CP_6-$FR_{80\%}$

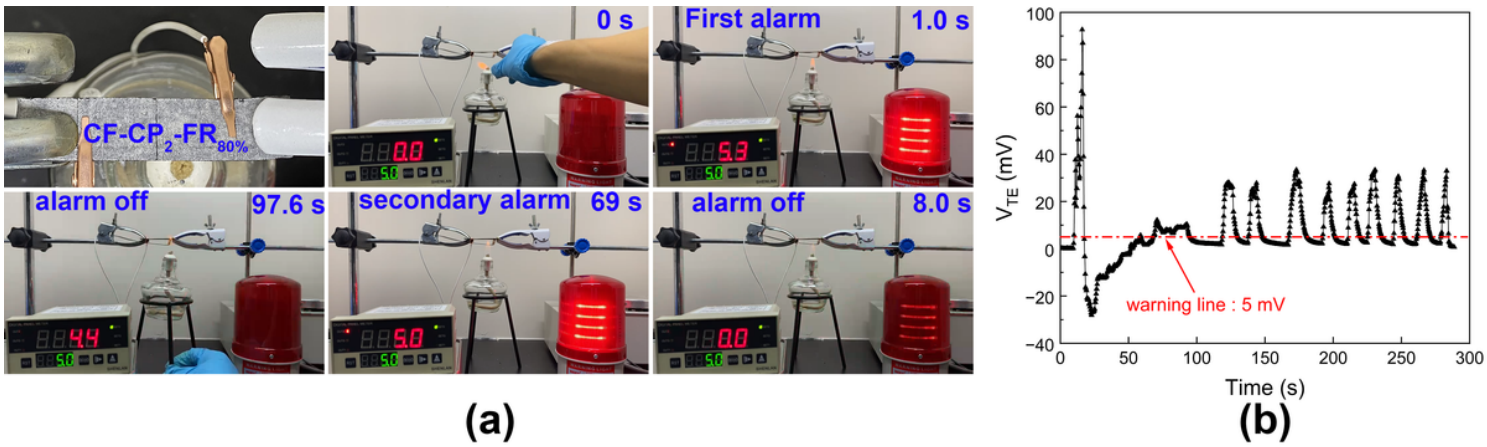

Figure 4

Fire warning performance of CF-CP_2-$FR_{80\%}$: (a)Video snapshots of the fire warning test process; (b) The corresponding real-time V_{TE} curve

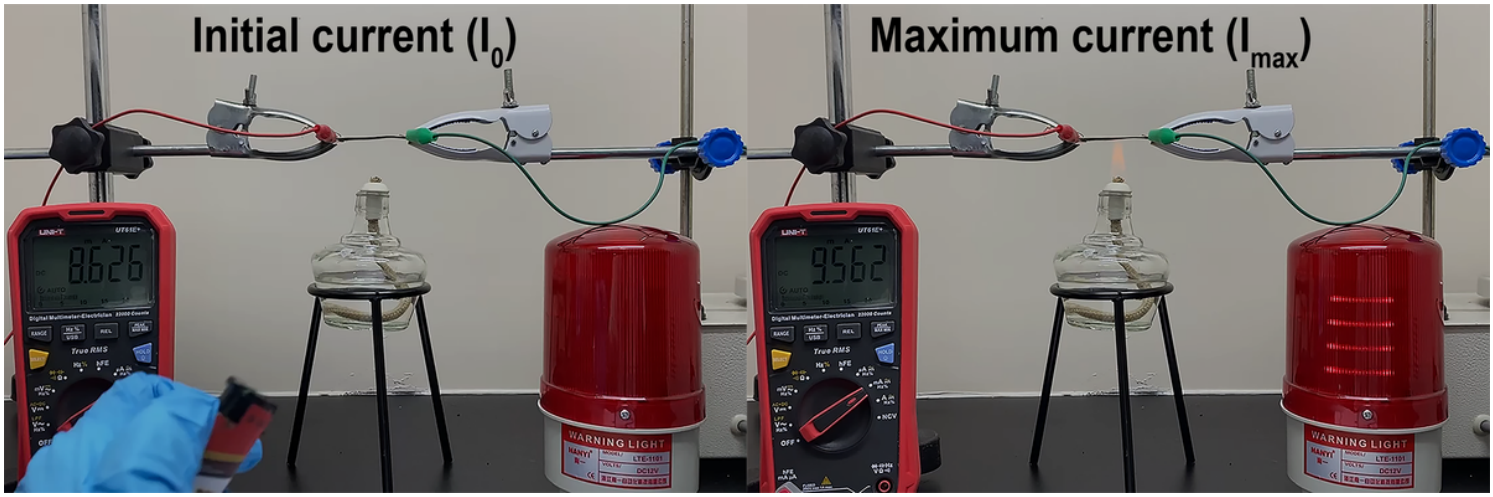

Figure 5

Video capture of the fire warning test process of CF-CP5-FR80%

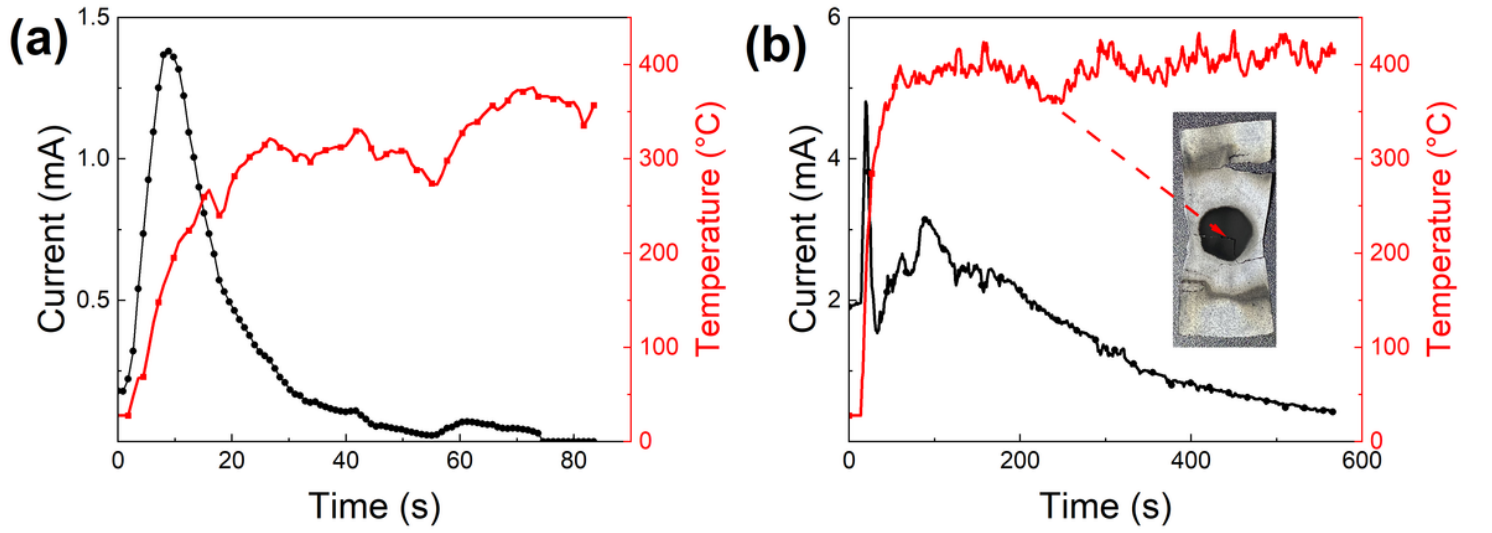

Figure 6

The real-time current curve at a fixed voltage of 12V: (a) CF-CP_3-$FR_{80\%}$ with a 1.5 cm wide cross-section, (b) CF-CP_3-$FR_{80\%}$ with a 3.0 cm wide cross-section

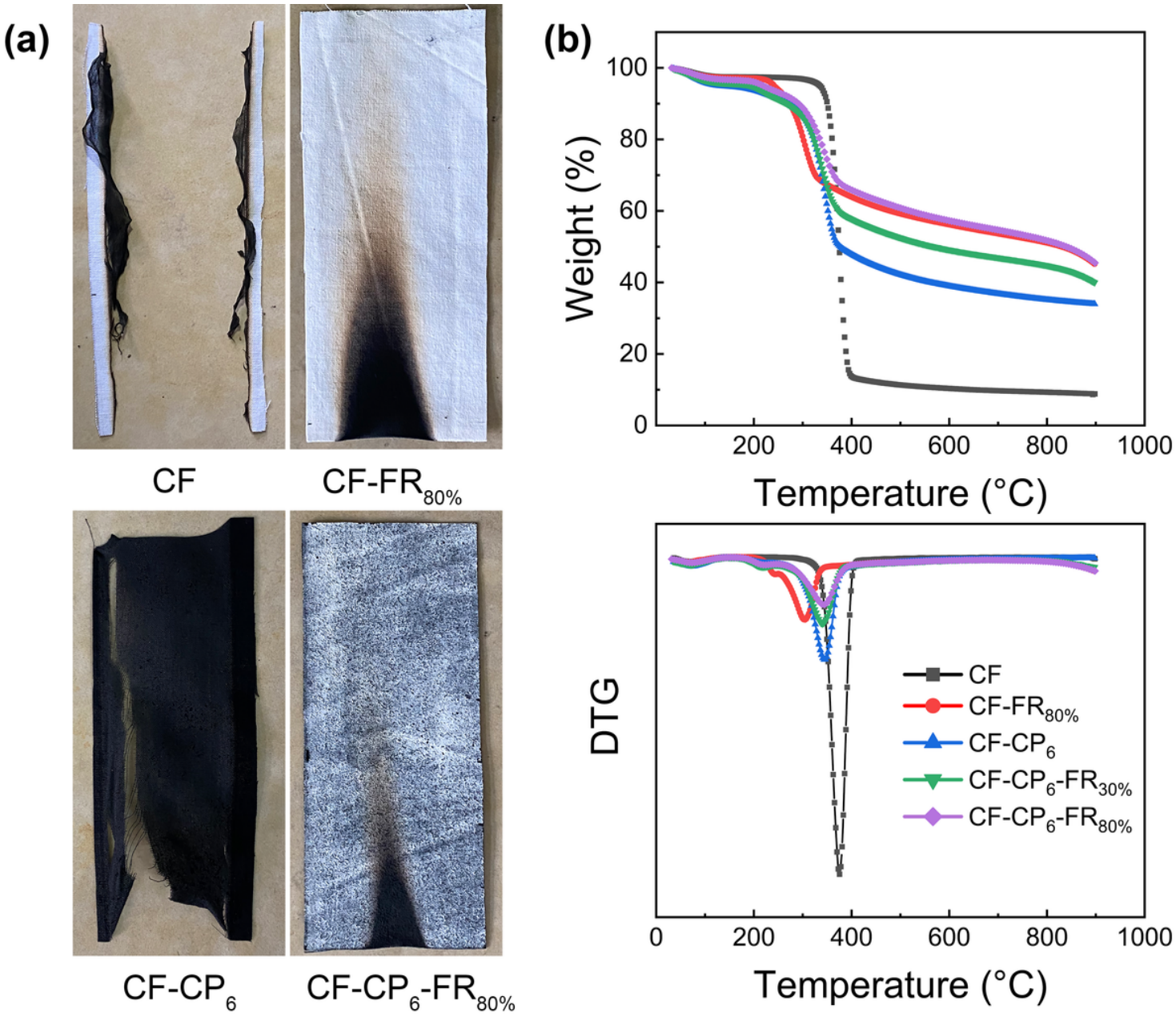

Figure 7

(a) Digital picture after VBT, (b) TG and DTG curves of CF, CF-$FR_{80\%}$, CF-CP_6, CF-CP_6-$FR_{30\%}$, and CF-CP_6-$FR_{80\%}$

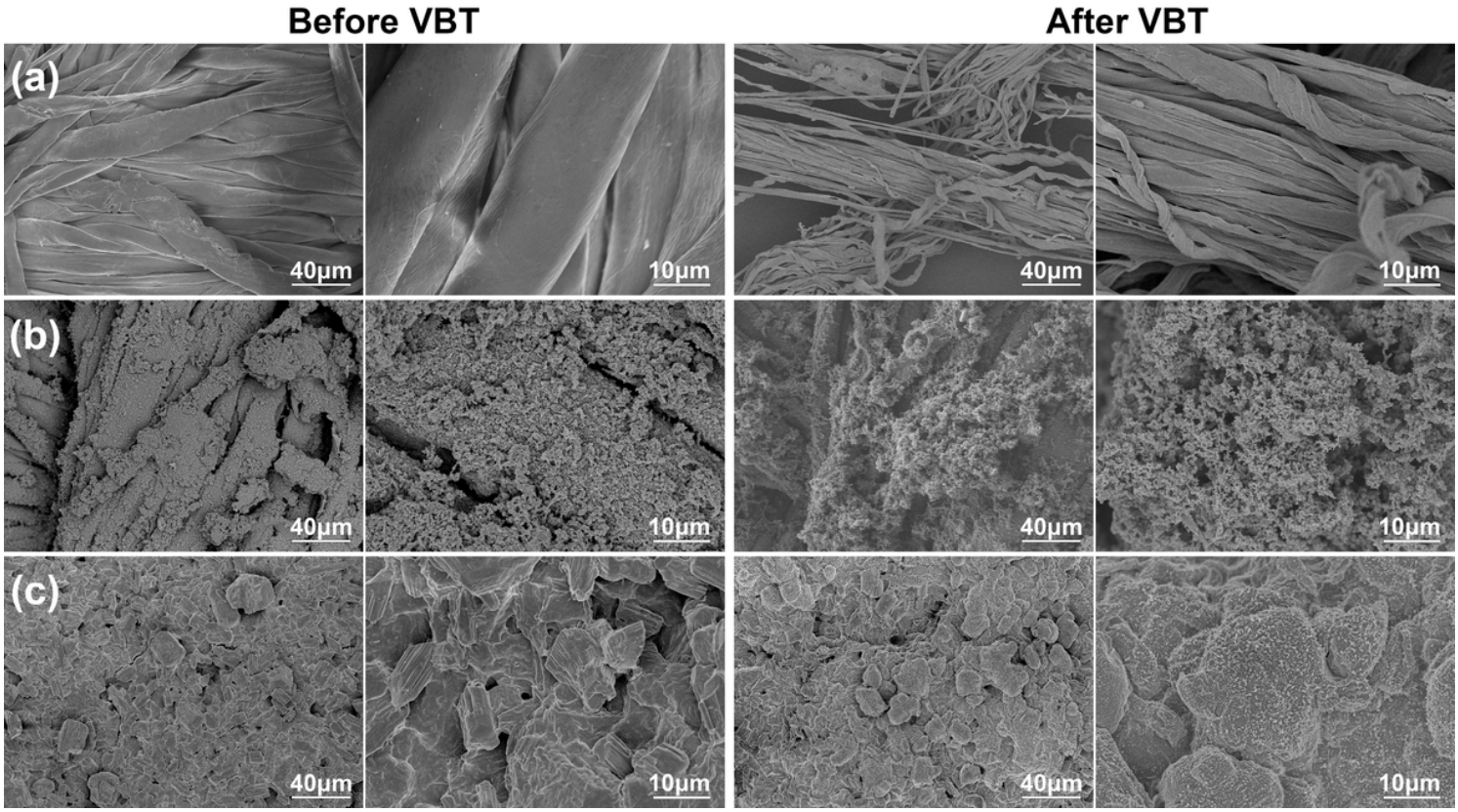

Figure 8

SEM image of (a) CF, (b) CF-CP_6, and (c) CF-CP_6-$FR_{80\%}$ before and after VBT

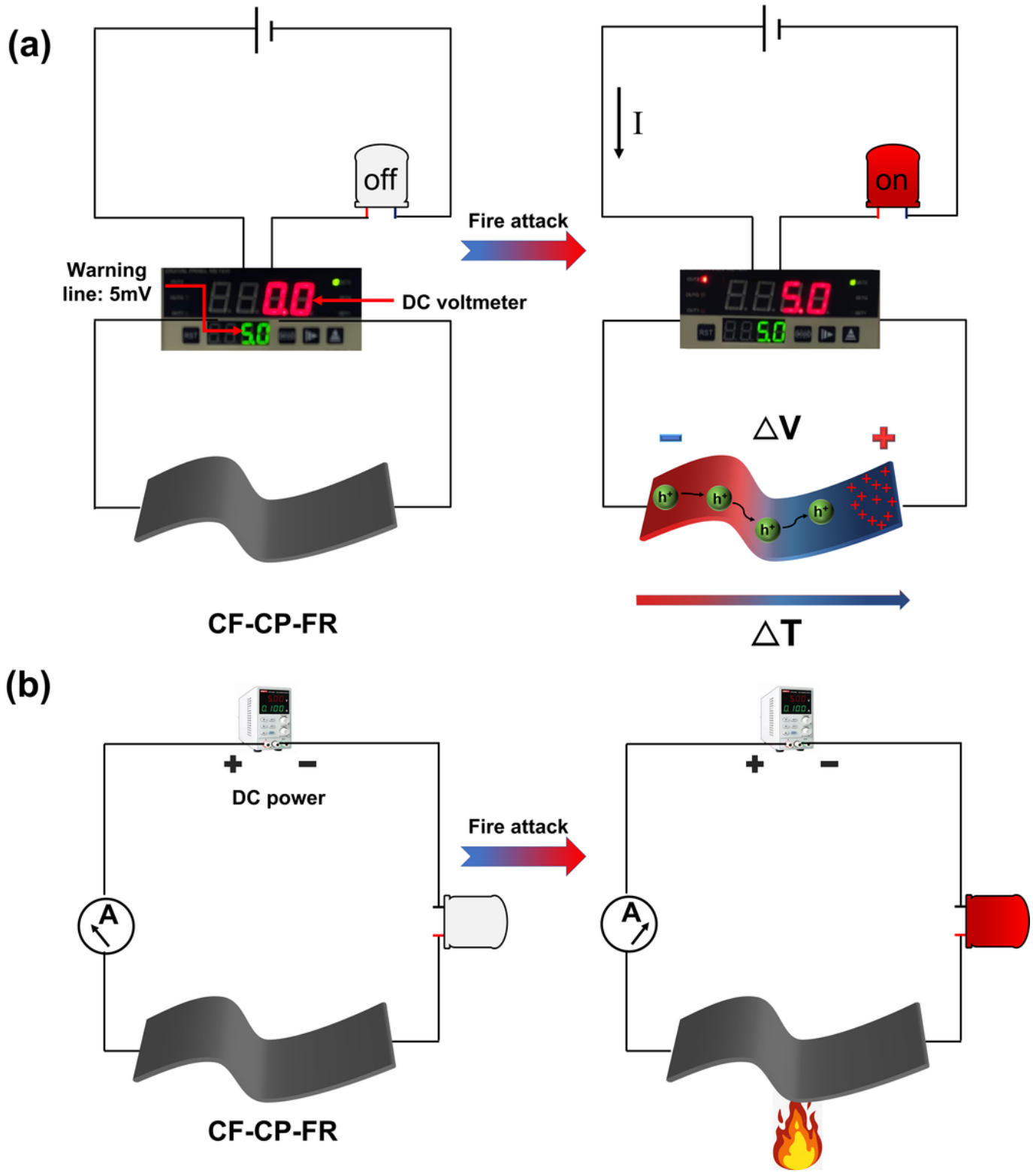

Figure 9

Schematic illustration of the fire warning process: (a) Thermoelectric fire-warning circuit, (b) thermal-resistance change-based fire warning circuit.

Supplementary Files

This is a list of supplementary files associated with this preprint. Click to download.

- GraphicalAbstarct.png
- Video1.mp4
- Video2.mp4
- Video3.mp4
- Video4.mp4